MOLECULAR & CELLULAR TOXICOLOGY, Vol. 3, No. 3, 198-207, September 2007

Application of Differential Expression of Genetic Profiles in Brain Tumors with Variable [^{18}F]-fluorodeoxyglucose Uptake

Seung-Ho Lee[1], **Mi-Jin Yun**[1], **Ki-Nam Kim**[1], **Sang-Hui Seo**[1], **Sung-Hwa Sohn**[1], **Yu-Ri Kim**[1], **Hye Won Kim**[1], **In Kyoung Kim**[1], **Boo Im Shim**[1], **Seung Min Lee**[1] **& Meyoung-Kon Kim**[1]

[1]Department of Biochemistry & Molecular Biology, College of Medicine, Korea University, Seoul 136-705, Korea
Correspondence and requests for materials should be addressed to M. K. Kim (jerrykim@korea.ac.kr)

Accepted 14 August 2007

Abstract

^{18}F-fluorodeoxyglucose (FDG) uptake on positron emission tomography (PET) scan has been found to reflect tumor aggressiveness and prognosis in various types of cancer. In this study, the gene expression profiles of glial tumors were evaluated to determine whether glial tumors with high ^{18}F-FDG uptake have more aggressive biological potential than with low uptake. Surgical specimens were obtained from the 12 patients with glial tumors (4 males and 8 females, age range 42-68 years). The tumor samples were divided into two groups based on the ^{18}F-FDG uptake PET scan findings: high ^{18}F-FDG uptake (n=4) and low ^{18}F-FDG uptake (n=8). The pathological tumor grade was closely correlated with the ^{18}F-FDG uptake pattern: Glial tumors with high ^{18}F-FDG uptake were pathologically Edmondson-Steiner grade III, while those with low uptake were grade II. The total RNA was extracted from the frozen tissues of all glial tumors (n=12), and adjacent non-cancerous tissue (n=3). The gene expression profiles were evaluated using cDNA microarray. The glial tumors with high ^{18}F-FDG uptake showed increase expression of 15 genes compared to those with low uptake ($P<$ 0.005). Nine genes were down-regulated. Gene expression is closely related to cell survival, cell-to-cell adhesion or cell spreading; therefore, glial tumors with high ^{18}F-FDG uptake appear to have more aggressive biological properties than those with low uptake.

Keywords: Glial tumors, ^{18}F-fluorodeoxyglucose uptake, Positron emission tomography, Gene expression profile, cDNA microarray

Cancer cells are known to show increased rates of glucose metabolism and on the basis of this, a positron emission tomography (PET) study using ^{18}F-fluorodeoxyglucose (^{18}F-FDG) has been used for the detection of primary and metastatic tumors[1]. FDG-PET is used in diagnostic oncology as a method of assessing the functional characteristics of solid tumors[2,3]. One of the first uses of FDG-PET was in brain tumor imaging[2]. In addition to assessment of FDG uptake in brain tumors using a visual grading scale[4], quantitative and semiquantitative measurements have been described in patients with brain tumors by comparing tumor uptake with that of normal areas of cortex or white matter[5]. The usefulness of FDG-PET scans has been reported extensively in patients with brain tumors, particularly malignant glioma[6]. This method, when used in a serial fashion, has been shown to provide both diagnostic and prognostic information in such patients[7,8]. Also, the degree of FDG-PET uptake has been shown to differentiate between radiation necrosis and recurrent tumor[9] and between benign and malignant neoplasia[5].

Recently, ^{18}F-FDG uptake on PET has been reported to be an important prognostic marker in various cancer, including non-small-cell lung cancer, head and neck cancer, lymphoma, pancreatic adenocarcinoma, and colorectal and cervical cancers[10-15], because tumors with higher ^{18}F-FDG uptake show higher cellular proliferation and are associated with a poorer survival rate than those with low ^{18}F-FDG uptake. The reduction of ^{18}F-FDG uptake after induction chemotherapy has been correlated with better disease-free and overall survival rates[16].

In glial tumors, the sensitivity of ^{18}F-FDG uptake PET is approximately 60%[17], which is considerably lower than that in ^{18}F-FDG avid tumors such as colorectal and lung cancers or lymphoma. The mechanisms underlying the low sensitivity of ^{18}F-FDG PET in glial tumors are uncertain. The facilitated diffusion of ^{18}F-FDG due to low expression of glucose transporter-1 (Glut-1)[18] and transport out of the cells due to unusually high expression of glucose-6-phosphatase have been considered as mechanisms of low ^{18}F-FDG uptake[17]. Previous studies, it has demonstrated that ^{18}F-FDG uptake is increased in poorly differentiated glial tumors and that clinical outcome is poorer in patients with a high tumor to non-tumor ^{18}F-FDG uptake ratio, indicating that ^{18}F-FDG uptake in glial

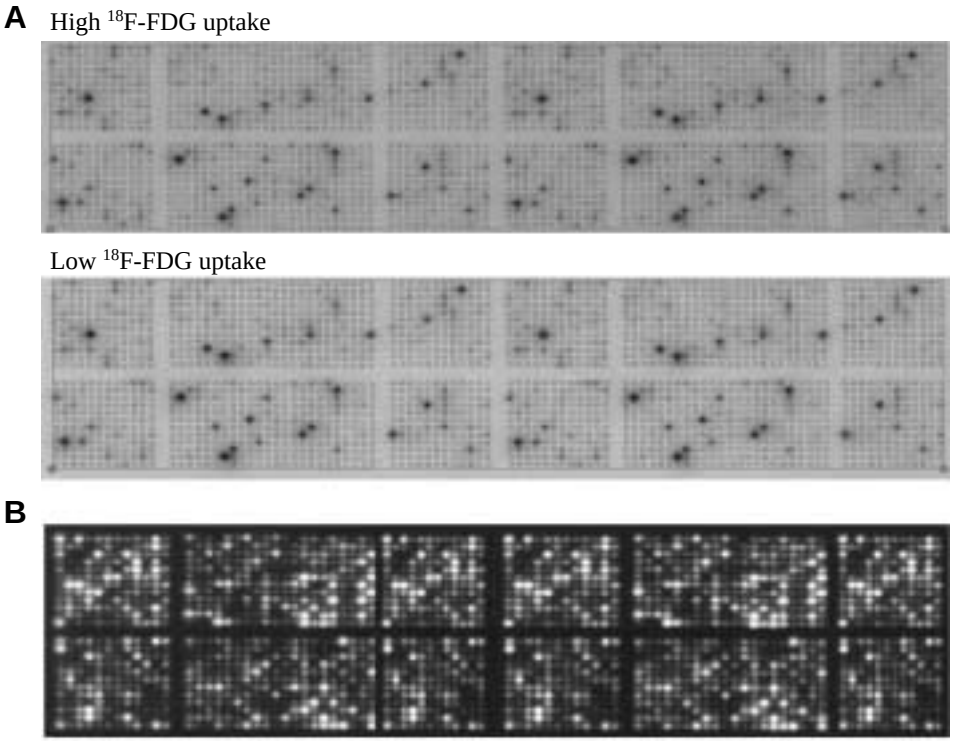

Figure 1. (A) Representative cDNA microarrays of two independent hybridization experiments comparing cDNAs generated from GBMs with high ^{18}F-FDG uptake (up) or from GBMs with low ^{18}F-FDG uptake[16]. The cDNA microarray contained the two sets of 1,152 genes and printed in duplicate (as indicated by the line), and each duplicate is composed of eight individual subarrays. (B) Superimposed image of primary images.

tumors is also closely related to tumor progression and prognosis[19].

In this study, we investigated the gene expression profiles of glial tumors with high ^{18}F-FDG uptake using cDNA microarray method, and compared with those of glial tumors with low ^{18}F-FDG uptake to evaluate whether the ^{18}F-FDG uptake pattern is correlated with tumor progression and metastatic potential at the molecular level.

Pathological Results in Relation to ^{18}F-FDG Uptake

The SUVs of the tumor ranged from 1.8 to 8.1 (4.6 $\pm$3.05) in the high uptake group and from 1.6 to 3.1 (2.2$\pm$0.47) in the low uptake group. The mean SUV of the non-tumor tissue was 1.8$\pm$1.21. Radioactive hybridization was visualized by phosphoimager technologies. The primary image, that is the results of primary capture by phosphoimager, is shown in Figure 1A. This particular array was printed in duplicate (as indicated by the line) and each duplicate was composed of eight individual subarrays. Visual inspection of the hybridization patterns readily identified a number of signals differentially expressed between normal and diseased tissue. Figure 1B is a superimposed image in which red color represents upregulation and green represents downregulation, and yellow represents genes of higher expression in high ^{18}F-FDG uptake and low ^{18}F-FDG uptake, such as housekeeping genes.

The tumors were divided into two groups as indicated by the microarray data, and the pathological grading of the tumor was closely correlated with the microarray clustering data and also with ^{18}F-FDG uptake patterns (Figure 2, Table 1): Glial tumors with high ^{18}F-FDG uptake were pathologically Edmondson -Steiner grade III, whereas those with low uptake were grade II.

The Microarray Data in Relation to ^{18}F-FDG Uptake

Analysis of the median densitometric signal intensity revealed that 24 genes differed between the patients of glial tumors with high ^{18}F-FDG uptake and low ^{18}F-FDG uptake by a Z-ratio of 2 at a descriptive $P \leq 0.05$. When the gene expression profiles in glial tumors with high ^{18}F-FDG uptake were compared to those with low uptake, 15 genes were up-regulated in the glial tumors with high ^{18}F-FDG uptake. In particular, genes related to tumor cell adhesion, invasion, metastasis or anti-tumoral immunity, such as insulin-like growth factor binding protein 2 (IGFBP2), mitogen-activated protein kinase, regulator of G-protein signalling 13 and prostaglandin-endoperoxide synthase 2 (prostaglandin G/H synthase and cyclooxygenase) were up-regulated. The human VEFG and rho

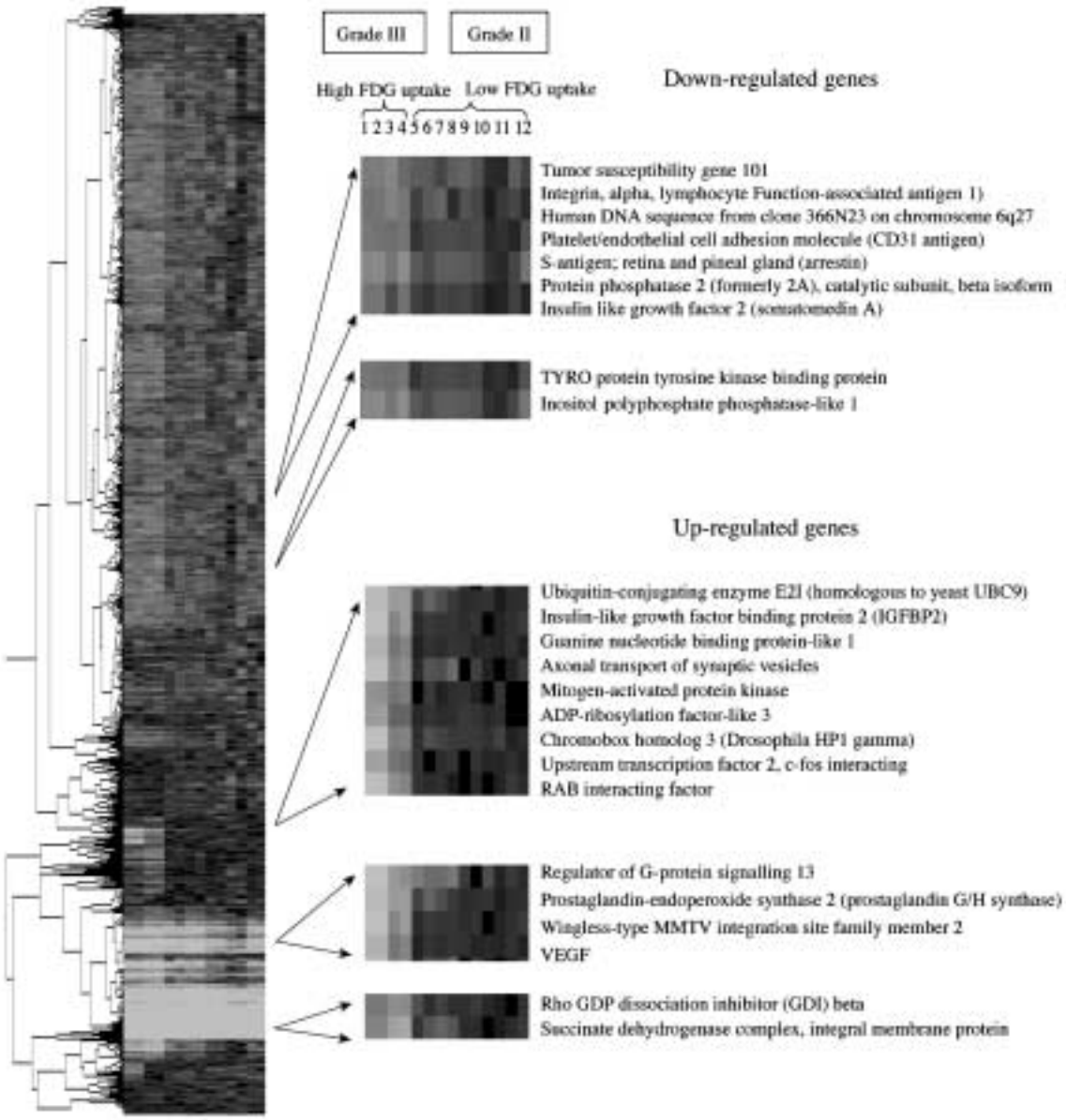

Figure 2. Clustergram of up- and down-regulated gene expression profile in the GBM with high ^{18}F-FDG uptake compared to those with low ^{18}F-FDG uptake. The dendrogram at the top indicates the pathological grading and ^{18}F-FDG uptake pattern appear to be well correlated. Four samples with high ^{18}F-FDG uptake were high-grade lesions, while all samples with low ^{18}F-FDG uptake were assigned to grade II.

GDP dissociation inhibitor (GDI) beta were also over -expressed. Nine genes, including tumor susceptibility gene 101, platelet/endothelial cell adhesion molecule (CD31 antigen), s-antigen; retina and pineal gland (arrestin) and protein phosphatase 2 (formerly 2A) catalytic subunit beta isoform were down-regulated (Figure 2).

The gene expression profiles are summarised in Table 2, 3. The results in Figure 3 show that the IGFBP2 protein and prostaglandin-endoperoxide synthase 2 were also elevated in the glial tumors with high ^{18}F-FDG uptake. Combining the results from cDNA array and RT-PCR, we accumulated comparable numbers of cases for each category. Elevation of IGFBP2 and prostaglandin-endoperoxide synthase 2 in the glial tumors with high ^{18}F-FDG uptake implies that the IGF and prostaglandin G/H synthase pathway are involved in glioma progression.

Discussion

^{18}F-FDG PET is a unique imaging method that provides *in vivo* evidence for both biochemical and physiological activities in the normal brain and spinal cord and in tumors that involve these structures[20]. It provides important information regarding tumor grade, extent of tumor, best sites for tumor biopsy, response to treatment, and prognosis. Because the brain derives its energy exclusively from glucose, ^{18}F-FDG is rapidly taken up in neuronal and glial cells through glucose transporter proteins, called GLUT-1, located on the membranous surface. ^{18}F-FDG is metabolized similarly to glucose and undergoes phosphorylation to FDG-6 phosphate. However, unlike glucose-6 phosphate, FDG-6 phosphate is trapped within the cell and cannot be metabolized further or, in the phosphorylated form, leave the cell. High-grade brain tumors accumulate ^{18}F-FDG more avidly than normal neurons, enabling their identification amid the background ^{18}F-FDG uptake in the brain. The intensity of ^{18}F-FDG uptake in brain tumors can be visually graded or quantified by metabolic activity ratios (Tmax/Gmean and Tmax/Wmean) using the uptake in the contralateral normal cortex and white matter as an internal standard[5,21,22]. These uptake measures have been validated in studies of ^{18}F-FDG-PET in both low- and high-grade brain tumors. Cutoff values (>0.8, 1.5, and 3, respectively, for Tmax/Gmean, Tmax/Wmean, and visual grade values) have been proposed that reliably could differentiate malignant from benign tumors[5].

Table 1. Clinical and ^{18}F-FDG PET findings of the GBM patients.

No	Age	Sex	Location	^{18}F-FDG uptake	Pathology	SUV
1	F	54	Right frontal	High	III	2.3
2	M	66	Right temporal	High	III	1.8
3	M	42	Left frontal	High	III	8.1
4	M	52	Pons	High	III	6.2
5	F	60	Right temporal	Low	II	2.3
6	F	54	Right frontal	Low	II	1.6
7	F	54	Right frontal	Low	II	2.4
8	M	68	Left temporal	Low	II	2.0
9	F	43	Left frontal	Low	II	1.8
10	M	47	Right frontal	Low	II	3.1
11	F	51	Right frontal	Low	II	2.5
12	F	50	Left frontal	Low	II	2.1

Glial tumor is the most common and most lethal primary malignant brain tumor. However, the role of ^{18}F-FDG PET in the initial diagnosis of glial tumors is limited because of its low sensitivity. In addition, the mechanisms involved in low ^{18}F-FDG uptake by glial tumors are controversial. Nevertheless, ^{18}F-FDG PET scan appears to be useful for predicting the clinical outcome and prognosis in glial tumor patients[17]. Therefore, it is important to assess the molecular biological findings in relation to ^{18}F-FDG uptake patterns.

Data on the correlation between proliferative activity and glycolysis in malignant tumors as measured by ^{18}F-FDG uptake have been reported in a small

Table 2. Up-regulated gene expression in the GBMs with high ^{18}F-FDG uptake compared to the GBMs with low ^{18}F-FDG uptake by cDNA array.

Gene name	Z-value[1)]		Z-difference[2)]	Z-ratio[3)]
	Low-	High-		
Ubiquitin-conjugating enzyme E2I (homologous to yeast UBC9)	−3.88	−0.53	3.35	4.26
Insulin-like growth factor binding protein 2 (IGFBP2)	−3.55	−0.42	3.13	3.98
Guanine nucleotide binding protein-like 1	−3.03	−0.07	2.96	3.76
Axonal transport of synaptic vesicles	−2.74	0.10	2.85	3.61
Mitogen-activated protein kinase	−3.06	−0.60	2.80	3.56
ADP-ribosylation factor-like 3	−3.09	−0.30	2.79	3.54
Chromobox homolog 3 (Drosophila HP1 gamma)	−2.95	−0.19	2.75	3.50
Upstream transcription factor 2, c-fos interacting	−3.02	−0.33	2.69	3.41
RAB interacting factor	−2.82	−0.19	2.62	3.33
VEGF	−2.04	0.27	2.30	2.92
Regulator of G-protein signalling 13	−2.00	0.18	2.18	2.77
Prostaglandin-endoperoxide synthase	−2.01	−0.04	1.98	2.51
Wingless-type MMTV integration site family member 2	−2.29	−0.33	1.96	2.49
Rho GDP dissociation inhibitor (GDI) beta	−1.92	0.02	1.94	2.46
Succinate dehydrogenase complex, integral membrane protein	−2.11	−0.18	1.93	2.44

[1)] $\text{Z-value}_{(\text{gene1})} = \log_{10}[\text{raw intensity}_{(\text{gene1})}] - \log_{10}[\text{mean raw intensity}_{(\text{all genes})}]/\text{standard deviation } \log_{10}[\text{raw intensity}_{(\text{all genes})}]$

[2)] $\text{Z-difference}_{(\text{gene1})} = \text{Z}_{(\text{gene1, array1})} - \text{Z}_{(\text{gene1, array2})}$

[3)] $\text{Z-ratio}_{(\text{gene1})} = \text{Z-difference}_{(\text{gene1})}/\text{Sdev}_{(\text{Z-difference all genes})}$

Table 3. Down-regulated gene expression in the GBMs with high ^{18}F-FDG uptake compared to the GBMs with low ^{18}F-FDG uptake by cDNA array.

Gene name	Z-value[1)]		Z-difference[2)]	Z-ratio[3)]
	Low-	High-		
Tumor susceptibility gene 101	0.08	−1.98	−2.06	−2.61
Integrin, alpha L (antigen CD11A (p180)	−0.42	−2.46	−2.03	−2.58
Human DNA sequence from clone 366N23 on chromosome 6q27	0.20	−1.79	−1.99	−2.53
Platelet/endothelial cell adhesion molecule (CD31 antigen)	−1.04	2.98	−1.95	−2.47
S-antigen; retina and pineal gland (arrestin)	−1.32	−3.24	−1.92	−2.44
Protein phosphatase 2 (formerly 2A), catalytic subunit, beta isoform	−0.67	−2.48	−1.81	−2.29
Insulin-like growth factor 2 (somatomedin A)	−0.56	−2.32	−1.76	−2.24
TYRO protein tyrosine kinase binding protein	−0.24	−1.98	−1.73	−2.20
Inositol polyphosphate phosphatase-like 1	−0.70	−2.39	−1.69	−2.15

[1)] $Z\text{-value}_{(gene1)} = \log_{10}[\text{raw intensity}_{(gene1)}] - \log_{10}[\text{mean raw intensity}_{(all\ genes)}]/\text{standard deviation } \log_{10}[\text{raw intensity}_{(all\ genes)}]$

[2)] $Z\text{-difference}_{(gene1)} = Z_{(gene1,\ array1)} - Z_{(gene1,\ array2)}$

[3)] $Z\text{-ratio}_{(gene1)} = Z\text{-difference}_{(gene1)} / Sdev_{(Z\text{-difference all genes})}$

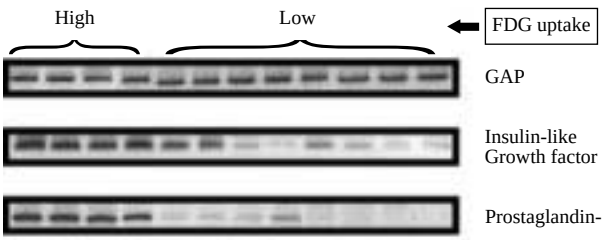

Figure 3. Representative RT-PCR data of insulin-like growth factor binding protein 2 and prostaglandin-endoperoxide synthase 2 in GBMs.

series of malignant lymphoma cases. Vesselle *et al.*[23] reported that ^{18}F-FDG uptake in non-small-cell lung cancer correlates with cellular proliferation assessed by Ki-67 immunohistochemistry. By contrast, the *in vitro* results of Higashi *et al.*[24] indicated no correlation between proliferative activity and ^{18}F-FDG uptake in a human ovarian adenocarcinoma cell line.

The molecular mechanisms and genetic alterations of glial tumorigenesis remain poorly understood, although the major environmental risk factors such as chemical carcinogens have been identified[25]. Recently, several studies have described the usefulness of DNA microarray in GBMs to profile global changes in gene expression and to identify the signature genes[26-30]: expression of the expressed gene 10, a number of other genes related to the cell cycle regulation, tumor metabolism or tissue invasion have been described in GBMs. However, there have been few consistently expressed genes, possibly due to the different analysis methods, the cDNAs selected for microarray or the conditions of the non-cancerous control tissues used for comparison.

In this study, numerous genes were differentially expressed in the glial tumors compared with the adjacent non-cancerous tissues, making it difficult to identity the novel signature genes related to the carcinogenesis or biological properties. Therefore, we focused on the differential gene expression between glial tumors with high ^{18}F-FDG uptake and those with low uptake on PET scan.

This study used a cDNA microarray with 1,152 human genes selected from the NCBI database. Fifteen genes were significantly up-regulated and nine were down-regulated in the glial tumors with high ^{18}F-FDG uptake. The gene expression of the IGFBP2, which appears to be associated with the formation of or progression to glial tumors, was markedly increased in glial tumors with high ^{18}F-FDG uptake. The IGFs stimulate cellular proliferation in an autocrine fashion in many tumors. It has been reported that human gliomas produce IGFs and express elevated levels of IGF receptors compared with normal brain tissue[31,32]. IGF also enhances three-dimensional growth of glioblastoma spheroids *in vitro*[33]. The effect of IGFs on cells is regulated by a family of IGFBPs[34-36], which can both attenuate and stimulate the mitogenic effect of IGFs[36,37]. Studies of the temporal and spatial expression of IGFBPs during development reveal that members of the IGFBP family are expressed in a tissue-specific and developmental stage-specific manner[38]. Unlike some of the other members, IGFBP2 is predominantly expressed in fetal tissues that are highly proliferative, such as the early postimplantation epiblast, the apical ectodermal ridge, and the progenitors of spleen and liver cells. In the nervous system, IGFBP2 is expressed in fetal astroglial cells. After birth, IGFBP2 expression significantly decreases in glial cells[39].

An association of IGFBP2 with several different

malignancies has been noted. Studies have shown that patients with prostate carcinoma have elevated serum IGFBP2 compared with patients with benign prostatic hyperplasia[40]. Increased expression of IGFBP2 was also found in malignant ovarian cyst fluid. Recently, it was shown that introduction of IGFBP2 expression increased tumorigenicity of recipient cells in a nude mouse xenograft model[41].

The expression of prostaglandin H synthase-2 (PHS) gene was slightly up-regulated. Prostaglandin H synthase (otherwise known as cyclooxygenase) is a key enzyme in the synthesis of prostaglandins and thromboxane. Two isoforms of PHS have been identified: constitutively expressed PHS-1, and mitogen-inducible PHS-2. Previous studies have demonstrated that PHS-2, but not PHS-1, is involved in colon carcinogenesis[42-44], and those nonsteroidal anti-inflammatory drugs (NSAIDs), which inhibit PHS, can reduce the risk of colon cancer[45]. Recently, constitutive expression of PHS-2 has also been demonstrated in various tumors in addition to colon cancer, such as skin, breast, lung, liver and pancreas carcinomas[46,47]. Furthermore, several studies have demonstrated the up-regulation of PHS-2 in transfection experiments of oncogenes[48-50], suggesting that up-regulation of PHS-2 could be a general phenomenon in carcinogenesis.

In brain tumors, elevated prostaglandin production and its correlation to anaplastic grade of glial tumors and meningiomas have been demonstrated[51]. Prostaglandins serve as autocrine and paracrine mediators and are involved in a variety of biological processes. A PHS-2 metabolite abundantly present in the lung cancer microenvironment, prostaglandin E2 (PGE2) is an important mediator of immunoregulation and epithelial survival. PGE2 exerts its multiple effects through four G protein-coupled receptors. It has been shown previously that GPCRs are able to trans-activate the epidermal growth factor receptor (EGFR) pathway leading to the promotion of cancer cell growth and motility[52,53]. Studies of human cancers have revealed the mechanisms of PGE2-mediated mitogen -activated protein kinase (MAPK) activation in non-small cell lung cancer (NSCLC) cells.

Based on these results, the gene expression profile of the glial tumors with high ^{18}F-FDG uptake on PET scan appears to have more aggressive nature than that of glial tumors with low ^{18}F-FDG uptake. The functional roles of the other genes demonstrated in our microarray results are not understood in relation to carcinogenesis or progression of glial tumors. Further studies will be required.

In conclusion, ^{18}F-FDG uptake pattern is closely correlated to the molecular markers involved in tumor progression and metastasis. GBMs with high ^{18}F-FDG uptake appear to have more aggressive biological properties than those with low uptake. Therefore, ^{18}F-FDG PET scan is an important diagnostic and prognostic tool in the evaluation of brain tumors, and gene expression profiling appears to be useful in understanding molecular characteristics of glial tumors with various FDG uptakes.

Methods

Patients

The study consisted of 12 patients with glial tumors (5 men, 7 women, aged 42-68 years; mean age 53.4 years) who underwent lobectomy. Brain tumors were classified on the basis of review hematoxilin and eosin stained sections of surgical specimens. All tumor samples were classified as World Health Organization (WHO) grade, and divided into two groups based on the PET scan findings; high uptake (n=4) and low uptake (n=8) (Table 1).

PET Studies

All patients fasted for at least 6 hours before the FDG-PET scans. Serum glucose levels were routinely obtained immediately before the scan and were found to be less than 140 mg/dL in all patients. PET scanning was performed using a GE advance PET scanner (GE advance, Milwaukee, WI, USA). PET image were acquired with the patients in the supine position, resting, with eyes closed. For attenuation correction, transmission scanning with 68Ge ring sources was performed for 7 min. Patients were injected with 370 MBq of ^{18}F-FDG intravenously. After 60 min, regional images of the brain were obtained for 20 min. Transaxial images were reconstructed using a filtered back projection and corrected for attenuation using the attenuation map obtained with the transmission images. The PET images were compared with the corresponding computed tomography (CT) or magnetic resonance (MR) images for accurate tumor localization, and the coronal, sagittal and axial image were qualitatively evaluated to assess whether the ^{18}F-FDG uptake in the tumor was or was not higher than that in surrounding non-cancerous brain cortex (high uptake group vs low uptake group, respectively).

Image Analysis

PET images were compared to compute tomography or magnetic resonance images to identify the tumor margin. Based on the anatomical information, the margins (regions of interest, ROIs) of the tumor lesion were manually drawn by an observer and then ^{18}F-FDG uptake was analyzed quantitatively by cal-

culating the standardized uptake value (SUV): SUV= (PET count × calibration factor)/(injection dose/body weight).

cDNA Microarray

Total RNA was extracted from the frozen tissues of 14 glial tumors using TRIzol (Invitrogen, Carlsbad, CA, USA). The RNA purity and integrity were confirmed by OD spectrophotometry and gel electrophoresis with a BioAnalyzer 2100 (Agilent Technologies, Inc., Palo Alto, CA, USA). Briefly, 3-10 μg RNA were labeled in a reverse transcription reaction containing 5× first strand PCR buffer, 1 μg of 24-mer poly dT primer, 4 μL of 20 mM each dNTP excluding dCTP, 4 μL of 0.1 M DTT, 40 U of RNase inhibitor, 6 μL of 3,000 Ci/mmol α-^{32}P dCTP to a final volume of 40 μL. The mixture was heated at 65˚C for 5 min, followed by incubation at 42˚C for 3 min. Two μL (specific activity: 200,000 U/mL) of Superscript II reverse transcriptase (Life Technologies) was then added and the samples were incubated for 30 min at 42˚C, followed by the addition of 2 μL of Superscript II reverse transcriptase and another 30 min of incubation. Five μL of 0.5 M EDTA was added to chelate divalent cations. After the addition of 10 μL of 0.1 M NaOH, the samples were incubated at 65˚C for 30 min to hydrolyze remaining RNA. Following the addition of 25 μL of 1 M Tris (pH 8.0), the samples were purified using Bio-Rad 6 purification columns (Hercules, CA). This resulted in 5×10^6 to 3×10^7 cpm per reaction[54].

Hybridization & Scanning

cDNA microarrays were pre-hybridized in hybridization buffer containing 4.0 mL Microhyb (Research Genetics), 10 μL of 10 mg/mL human Cot 1 DNA (Life Technologies), and 10 μL of 8 mg/mLpoly dA (Pharmacia, NJ). Both Cot 1 and poly dA were denatured at 95˚C for 5 min prior to use. After 4 h of prehybridization at 42˚C, approximately 10^7 cpm/mL of heat-denatured (95˚C, 5 min) probes were added and incubation was continued for 17 h at 42˚C. Hybridized arrays were washed three times in 2× SSC and 0.1% SDS for 15 min at room temperature. The microarrays were exposed to phosphorimager screens for 1-5 days, and the screens were then scanned in a FLA -8000 (Fuji Photo Film Co) at 50 μm resolution[54].

Data Analysis

Microarray images were trimmed and rotated for further analysis using L-Processor (Fuji Photo Film Co). Gene expression of each microarrays was captured by the intensity of each spot produced by radioactive isotopes. Pixels per spot were counted by Arrayguage (Fuji Photo Film Co) and were exported to Microsoft Excel (Microsoft, Seattle, WA). The data were normalized with Z transformation to obtain Z scores by subtracting each average of gene intensity and dividing with each standard deviation. Z scores provide each of 2,304 genes with the distance from the average intensity and were expressed in units of standard deviation. Thus, each Z score provides flexibility to compare different sets of microarray experiments by adjusting differences in hybridization intensities.

Gene expression difference as compared to untreated control cells was calculated by comparing the Z score differences (Z differences) among the same genes. This facilitates to compare each gene that had been up- or down-regulated as compared to the control cells. Z differences were calculated first by subtracting Z scores of the control from each Z score of the samples. These differences were normalized again to distribute their position by subtracting the average Z difference and dividing with the standard deviation of the Z differences. These distributions represent the Z ratio value, and provide the efficiency for comparing each microarray experiment[54].

Scatter plots of intensity values were produced by Spotfire (Spotfire, Inc., Cambridge, MA)[55]. Cluster analysis was performed on Z-transformed microarray data by using two programs available as shareware from Michael Eisen's laboratory (http://rana.lbl.gov). Clustering of changes in gene expression was determined by using public domain Cluster based on pair wise complete-linkage cluster analysis[56].

Validation of Microarray Data with RT-PCR

Two genes detected on the microarray data were selected for the validation of microarray results. The total RNA was extracted from 60 μg frozen tissue of each glial tumors using TRIzol (Invitrogen, Carlsbad, CA, USA). Reverse transcription for cDNA was performed from 5 μg total RNA using 2 μg random hexamer (Amersham Pharmacia Biotech, Inc., Uppsala, Sweden), 1.25 mM dNTP (Boehringer-Mannheim, Mannheim, Germany) and 200 UM-MLV reverse transcriptase (Gibco BRL, Grand Island, NY, USA). PCR was performed using 0.25 mM dNTP, 0.25 U Taq polymerase (Perkin Elmer, Norwalk, CT, USA), 10 pmol primer pairs and 3 μL cDNA with a thermal cycler. The following primer pairs were used for IGFBP2, prostaglandin-endoperoxide synthase 2 and GAPDH amplification: IGFBP2, 5′-AGCCCCTCA-AGTCGGGTA (sense), 5′-TGCGGTCTACTGCAT-CCG (antisense); prostaglandin-endoperoxide synthase 2, 5′-CAGAGTATGCGATGTGCTTA (sense), 5′-GCCAGTGATAGAGGGTGTTA (antisense);

GAPDH, 5′-CGGGAAGCTTGTGATCAATGG-3 (sense), 5′-GGCAGTGATGGCATGGAC-TG-3′ (antisense).

Acknowledgements

This study was supported by a grant from Medical Research Center for Environmental Toxicogenomic and Proteomics, funded by Korea Science and Engineering Foundations and Ministry of Science & Technology, a grant from the Korea Health 21 R & D Project, Ministry of Health and Welfare, R. O. K (Hmp-00-GN-01-0002 & 03-PJ10-PG13-GD01-0002), a Korea Institute of Science & Technology Evaluation and Planning (KISTEP) and Ministry of Science & Technology (MOST), Korean government, through its National Nuclear Technology Program, and a grant No. R01-2001-000-00212-0 from the Basic Research Program of the Korea Science & Engineering Foundation.

References

1. Hoh, C. K. *et al*. PET in oncology: will it replace the other modalities? *Semin Nucl Med* **27**:94-106 (1997).
2. Di Chiro, G. *et al*. Issues in the in vivo measurement of glucose metabolism of human central nervous system tumors. *Ann Neurol* **15**:S138-146 (1984).
3. Hagge, R. J., Wong, T. Z., & Coleman, R. E. Positron emission tomography: brain tumors and lung cancer. *Radiol Clin North Am* **39**:871-881 (2001).
4. Kim, C. K., Alavi, J. B., Alavi, A. & Reivich, M. New grading system of cerebral gliomas using positron emission tomography with F-18 fluorodeoxyglucose. *J Neurooncol* **10**:85-91 (1991).
5. Delbeke, D. *et al*. Optimal cutoff levels of F-18 fluorodeoxyglucose uptake in the differentiation of low-grade from high-grade brain tumors with PET. *Radiology* **195**:47-52 (1995).
6. De Witte, O. *et al*. Prognostic value positron emission tomography with [^{18}F]fluoro-2-deoxy-D-glucose in the low-grade glioma. *Neurosurgery* **39**:470-476; discussion 476-477 (1996).
7. Barker, F. G. *et al*. 18-Fluorodeoxyglucose uptake and survival of patients with suspected recurrent malignant glioma. *Cancer* **79**:115-126 (1997).
8. Schifter, T. *et al*. Serial FDG-PET studies in the prediction of survival in patients with primary brain tumors. *J Comput Assist Tomogr* **17**:509-561 (1993).
9. Chao, S. T. *et al*. The sensitivity and specificity of FDG PET in distinguishing recurrent brain tumor from radionecrosis in patients treated with stereotactic radiosurgery. *Int J Cancer* **96**:191-197 (2001).
10. Vansteenkiste, J. F. *et al*. Prognostic importance of the standardized uptake value on (18)F-fluoro-2-deoxy-glucose-positron emission tomography scan in non-small-cell lung cancer: An analysis of 125 cases. Leuven Lung Cancer Group. *J Clin Oncol* **17**:3201-3206 (1999).
11. Halfpenny, W. *et al*. A possible prognostic factor in head and neck cancer. *Br J Cancer* **86**:512-516 (2002).
12. Spaepen, K. *et al*. Prognostic value of pretransplantation positron emission tomography using fluorine 18-fluorodeoxyglucose in patients with aggressive lymphoma treated with high-dose chemotherapy and stem cell transplantation. *Blood* **102**:53-59 (2003).
13. Nakata, B. *et al*. ^{18}F-fluorodeoxyglucose positron emission tomography and the prognosis of patients with pancreatic adenocarcinoma. *Cancer* **79**:695-699 (1997).
14. Burt, B. M. *et al*. Using positron emission tomography with [(18)F]FDG to predict tumor behavior in experimental colorectal cancer. *Neoplasia* **3**:189-195 (2001).
15. Miller, T. R., Pinkus, E., Dehdashti, F. & Grigsby, P. W. Improved prognostic value of ^{18}F-FDG PET using a simple visual analysis of tumor characteristics in patients with cervical cancer. *J Nucl Med* **44**:192-197 (2003).
16. Downey, R. J. *et al*. Whole body ^{18}FDG-PET and the response of esophageal cancer to induction therapy: results of a prospective trial. *J Clin Oncol* **21**:428-432 (2003).
17. Chung, J. K., *et al*. Comparison of [^{18}F]fluorodeoxyglucose uptake with glucose transporter-1 expression and proliferation rate in human glioma and non-small-cell lung cancer. *Nucl Med Commun* **25**:11-17 (2004).
18. Meyer, P. T. *et al*. High F-18 FDG uptake in a low-grade supratentorial ganglioma: a positron emission tomography case report. *Clin Nucl Med* **25**:694-697 (2000).
19. Lee, J. K., Liu, R. S., Shiang, H. R. & Pan, D. H. Usefulness of semiquantitative FDG-PET in the prediction of brain tumor treatment response to gamma knife radiosurgery. *J Comput Assist Tomogr* **27**:525-529 (2003).
20. Wong, T. Z., van der Westhuizen, G. J. & Coleman, R. E. Positron emission tomography imaging of brain tumors. *Neuroimaging Clin N Am* **12**:615-626 (2002).
21. Hoffman, J. M. *et al*. FDG-PET in pediatric posterior fossa brain tumors. *J Comput Assist Tomogr* **16**:62-68 (1992).
22. Meyer, P. T. *et al*. Comparison of visual and ROI-based brain tumour grading using ^{18}F-FDG PET: ROC analyses. *Eur J Nucl Med* **28**:165-174 (2001).
23. Vesselle, H. *et al*. Lung cancer proliferation correlates with [F-18]fluorodeoxyglucose uptake by positron emission tomography. *Clin Cancer Res* **6**:3837-3844 (2000).
24. Higashi, K., Clavo, A. C. & Wahl, R. L. Does FDG

uptake measure proliferative activity of human cancer cells? *In vitro* comparison with DNA flow cytometry and tritiated thymidine uptake. *J Nucl Med* **34**:414-419 (1993).
25. Chen, C. C. Protein kinase C alpha, delta, epsilon and zeta in C6 glioma cells. TPA induces translocation and down-regulation of conventional and new PKC isoforms but not atypical PKC zeta. *FEBS Lett* **332**: 169-173 (1993).
26. Bredel, M. *et al*. Functional network analysis reveals extended gliomagenesis pathway maps and three novel MYC-interacting genes in human gliomas. *Cancer Res* **65**:8679-8689 (2005).
27. Mischel, P. S., Cloughesy, T. F. & Nelson, S. F. DNA-microarray analysis of brain cancer: molecular classification for therapy. *Nat Rev Neurosci* **5**:782-792 (2004).
28. Sallinen, S. L. *et al*. Identification of differentially expressed genes in human gliomas by DNA microarray and tissue chip techniques. *Cancer Res* **60**: 6617-6622 (2000).
29. Fuller, G. N. *et al*. Reactivation of insulin-like growth factor binding protein 2 expression in glioblastoma multiforme: a revelation by parallel gene expression profiling. *Cancer Res* **59**:4228-4232 (1999).
30. Hoelzinger, D. B. *et al*. Gene expression profile of glioblastoma multiforme invasive phenotype points to new therapeutic targets. *Neoplasia* **7**:7-16 (2005).
31. Glick, R. P., Unterman, T. G., Van der Woude, M. & Blaydes, L. Z. Insulin and insulin-like growth factors in central nervous system tumors. Part V: Production of insulin-like growth factors I and II *in vitro*. *J Neurosurg* **77**:445-450 (1992).
32. Sandberg-Nordqvist, A. C. *et al*. Characterization of insulin-like growth factor 1 in human primary brain tumors. *Cancer Res* **53**:2475-2478 (1993).
33. Morford, L. A., Boghaert, E. R., Brooks, W. H. & Roszman, T. L. Insulin-like growth factors (IGF) enhance three-dimensional (3D) growth of human glioblastomas. *Cancer Lett* **115**:81-90 (1997).
34. Jones, J. I. & Clemmons, D. R. Insulin-like growth factors and their binding proteins: biological actions. *Endocr Rev* **16**:3-34 (1995).
35. Ranke, M. B. & Elmlinger, M. Functional role of insulin-like growth factor binding proteins. *Horm Res* **48**(4): 9-15 (1997).
36. Zapf, J. Physiological role of the insulin-like growth factor binding proteins. *Eur J Endocrinol* **132**:645-654 (1995).
37. Blum, W. F. *et al*. Insulin-like growth factor I (IGF-I)-binding protein complex is a better mitogen than free IGF-I. *Endocrinology* **125**:766-772 (1989).
38. Cerro, J. A., Grewal, A., Wood, T. L. & Pintar, J. E. Tissue-specific expression of the insulin-like growth factor binding protein (IGFBP) mRNAs in mouse and rat development. *Regul Pept* **48**:189-198 (1993).
39. Wood, T. L., Streck, R. D. & Pintar, J. E. Expression of the IGFBP-2 gene in post-implantation rat embryos. *Development* **114**:59-66 (1992).
40. Ho, P. J. & Baxter, R. C. Insulin-like growth factor-binding protein-2 in patients with prostate carcinoma and benign prostatic hyperplasia. *Clin Endocrinol (Oxf)* **46**:333-342 (1997).
41. Menouny, M., Binoux, M. & Babajko, S. IGFBP-2 expression in a human cell line is associated with increased IGFBP-3 proteolysis, decreased IGFBP-1 expression and increased tumorigenicity. *Int J Cancer* **77**:874-879 (1998).
42. Eberhart, C. E. *et al*. Up-regulation of cyclooxygenase 2 gene expression in human colorectal adenomas and adenocarcinomas. *Gastroenterology* **107**:1183-1188 (1994).
43. Kutchera, W. *et al*. Prostaglandin H synthase 2 is expressed abnormally in human colon cancer: evidence for a transcriptional effect. *Proc Natl Acad Sci USA* **93**:4816-4820 (1996).
44. Sano, H. *et al*. Expression of cyclooxygenase-1 and -2 in human colorectal cancer. *Cancer Res* **55**:3785-3789 (1995).
45. Smalley, W. E. & DuBois, R. N. Colorectal cancer and nonsteroidal anti-inflammatory drugs. *Adv Pharmacol* **39**:1-20 (1997).
46. Hida, T. *et al*. Increased expression of cyclooxygenase 2 occurs frequently in human lung cancers, specifically in adenocarcinomas. *Cancer Res* **58**:3761-3764 (1998).
47. Tucker, O. N. *et al*. Cyclooxygenase-2 expression is up-regulated in human pancreatic cancer. *Cancer Res* **59**:987-990 (1999).
48. Sheng, G. G. *et al*. A selective cyclooxygenase 2 inhibitor suppresses the growth of H-ras-transformed rat intestinal epithelial cells. *Gastroenterology* **113**: 1883-1891 (1997).
49. Subbaramaiah, K. *et al*. Transcription of cyclooxygenase-2 is enhanced in transformed mammary epithelial cells. *Cancer Res* **56**:4424-4429 (1996).
50. Zhang, X., Morham, S. G., Langenbach, R. & Young, D. A. Malignant transformation and antineoplastic actions of nonsteroidal antiinflammatory drugs (NSAIDs) on cyclooxygenase-null embryo fibroblasts. *J Exp Med* **190**:451-459 (1999).
51. Butti, G. *et al*. A study on the biological behavior of human brain tumors. Part II: Steroid receptors and arachidonic acid metabolism. *J Neurooncol* **10**:241-246 (1991).
52. Pai, R. *et al*. Prostaglandin E2 transactivates EGF receptor: a novel mechanism for promoting colon cancer growth and gastrointestinal hypertrophy. *Nat Med* **8**:289-293 (2002).
53. Buchanan, F. G., Wang, D., Bargiacchi, F. & DuBois, R. N. Prostaglandin E2 regulates cell migration via the intracellular activation of the epidermal growth factor receptor. *J Biol Chem* **278**:35451-35457 (2003).
54. Vawter, M. P. *et al*. Application of cDNA microarrays to examine gene expression differences in schizophrenia. *Brain Res Bull* **55**:641-650 (2001).

55. Tanaka, T. S. *et al*. Genome-wide expression profiling of mid-gestation placenta and embryo using a 15,000 mouse developmental cDNA microarray. *Proc Natl Acad Sci* **97**:9127-9132 (2000).

56. Eisen M. B., Spellman P. T., Brown P. O. & Botstein D. Cluster analysis and display of genome-wide expression patterns. *Proc Natl Acad Sci* **95**:14863-14868 (1998).